Electronic Supplementary Material (ESI) for RSC Advances.

Supporting Information

Three dimensional graphdiyne-like porous triptycene network for gas adsorption and separation

Hui Ma,[a] Bin-Bin Yang,[a] Zhen Wang,[a] Kai Wu[b*] and Chun Zhang[a*]

[a]College of Life Science and Technology, National Engineering Research Center for Nanomedicine, Huazhong University of Science and Technology, Wuhan, 430074, China.
[b]Technology R&D Center, Hubei Tobacco (Group) Co., Ltd., Wuhan, 430070, China.

Instruments

FT-IR spectrum was acquired using the Thermo Scientific Nicolet iS50R fourier transform infrared spectrometer in the range of 400-4000 cm^{-1} with the KBr disc. Liquid ^{1}H-NMR spectra were conducted on the Bruker AscendTM 600 MHZ spectrometer at resonance frequencies of 600 MHz. SEM photos were captured on a FEI Sirion 200 scanning electron microscope. TEM images were collected on a FEI Tecnai G2 20 transmission electron microscope. TGA plot was obtained using the PerkinElmer Instruments Pyris1 thermogravimetric analyzer under nitrogen at a heating rate of 10 °C min^{-1} from 30 °C to 800 °C. PXRD pattern was collected on a PANalytical B.V. Empyrean X-ray powder diffractometer using Cu Kα radiation. Surface area and pore size distributions were measured by nitrogen adsorption and desorption at 77 K using a Micromeritics ASAP 2020 volumetric adsorption analyzer. Sample was degassed at 120 °C for 8 h under vacuum before analysis. CO_2 isotherms were measured at 273 and 298 K up to 1.0 bar using a Micromeritics ASAP 2020 volumetric adsorption analyzer with the same degassing procedure.

The synthesis of monomer

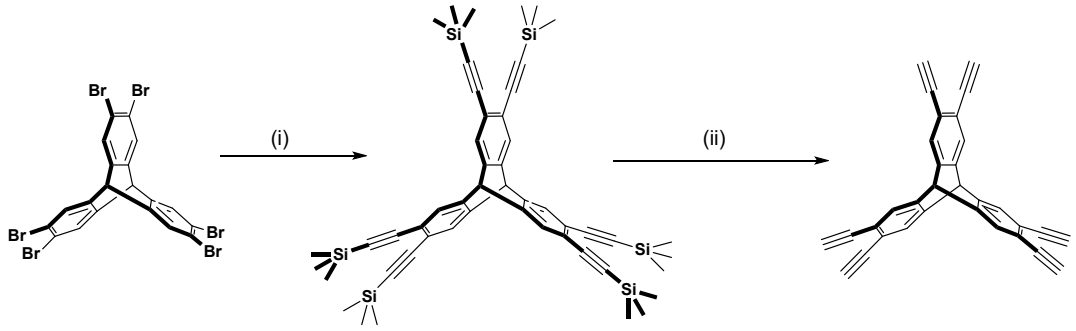

Scheme S1 Synthesis of 2,3,6,7,14,15-hexaethynyltriptycene. (i) TMSA, $Pd(PPh_3)_2Cl_2$, PPh_3, CuI, TEA, 70 °C, 24 h; (ii) TBAF, CH_2Cl_2, 25 °C, 6 h.

2,3,6,7,14,15-Hexakis(trimethylsilylethynyl)triptycene: Hexabromotriptycene (510 mg, 0.70 mmol), CuI (85 mg, 0.45 mmol), triphenylphosphine (220 mg, 0.85 mmol) and $PdCl_2(PPh_3)_2$ (280 mg, 0.40 mmol) were weighed and placed in a 50 mL two necked round-bottomed flask. Then the mixture and trimethylsilylacetylene (3 mL, 21.23 mmol) were dissolved in triethylamine (25 mL) under an argon atmosphere and heated at 70 °C overnight. After cooling down to room temperature, the solvent was removed under reduced pressure, the residue was dissolved in dichloromethane and filtered through silica. The product was obtained by chromatography with silica gel (petroleum ether/dichloromethane = 10/1, v/v) as white powders (432 mg, 0.52 mmol, 74%). ^{1}H NMR (600 MHz, $CDCl_3$) δ = 7.42 (s, 6H), 5.23 (s, 2H), 0.26 (s, 54H) ppm. ^{13}C NMR (150 MHz, $CDCl_3$) δ = 143.29, 127.44, 123.41, 103.12, 98.23, 52.49, 0.01 ppm. HRMS calcd. for $C_{50}H_{62}Si_6$ [M+], *m/z* = 830.3467; found 830.3481.

2,3,6,7,14,15- Hexaethynyltriptycene: The synthesized hexakis(trimethylsilylethynyl)triptycene (302 mg, 0.36 mmol) was dissolved in tetrahydrofuran (9 mL), and tetrabutylammonium fluoride (1 M in THF, 3 mL, 3 mmol) was added. The mixture was stirred under room temperature and monitored by TLC (petroleum ether/ ethyl acetate = 4/1, v/v). As the reaction completed, the solvent was removed under reduced pressure, and the product was purified through chromatography with silica gel (petroleum ether/ ethyl acetate = 4/1, v/v) as yellow powders (103 mg, 0.26 mmol, 72%). ^{1}H NMR (600 MHz, $CDCl_3$) δ = 7.53 (s, 6H), 5.37 (s, 2H), 3.29 (s, 6H) ppm. ^{13}C NMR (150 MHz, $CDCl_3$) δ = 143.60, 127.91, 122.94, 81.61, 81.02, 52.36 ppm. HRMS calcd. for $C_{32}H_{15}$ [M+], *m/z* = 398.1168; found 398.1168.

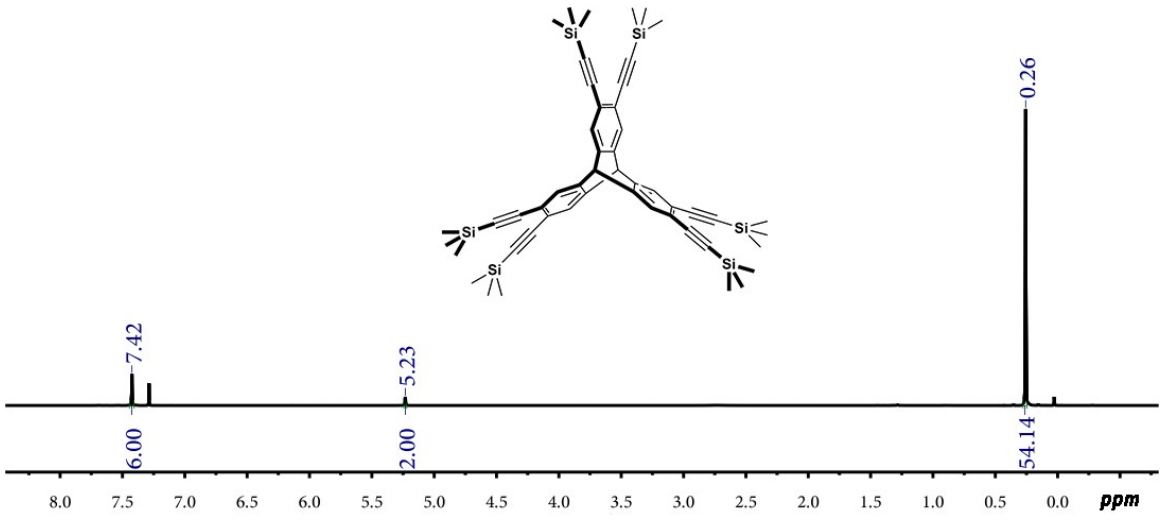

Fig. S1 ^{1}H NMR spectrum of 2,3,6,7,14,15-Hexakis(trimethylsilylethynyl)triptycene.

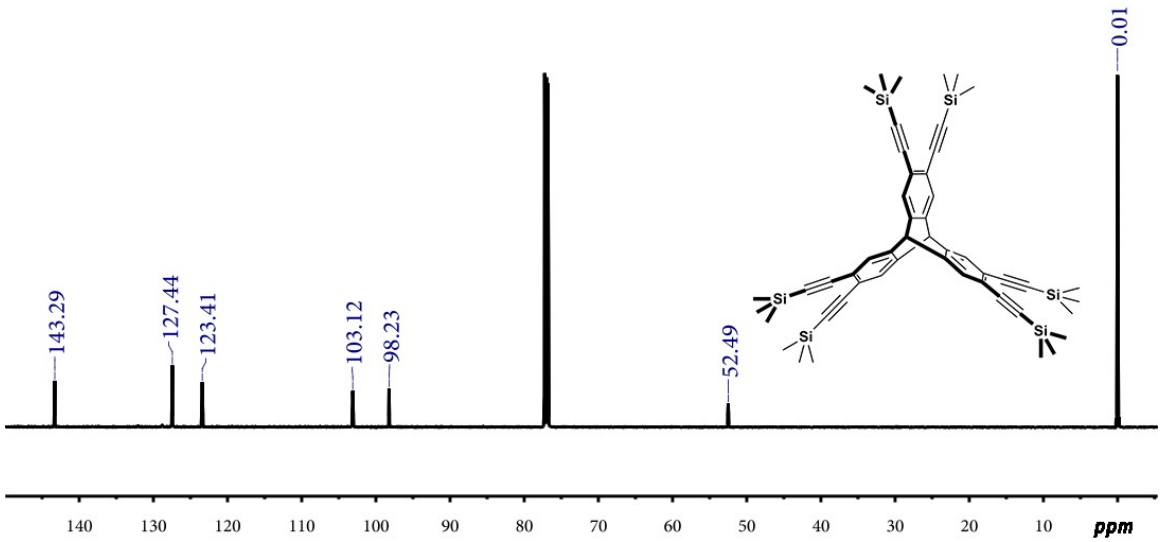

Fig. S2 ^{13}C NMR spectrum of 2,3,6,7,14,15-Hexakis(trimethylsilylethynyl)triptycene.

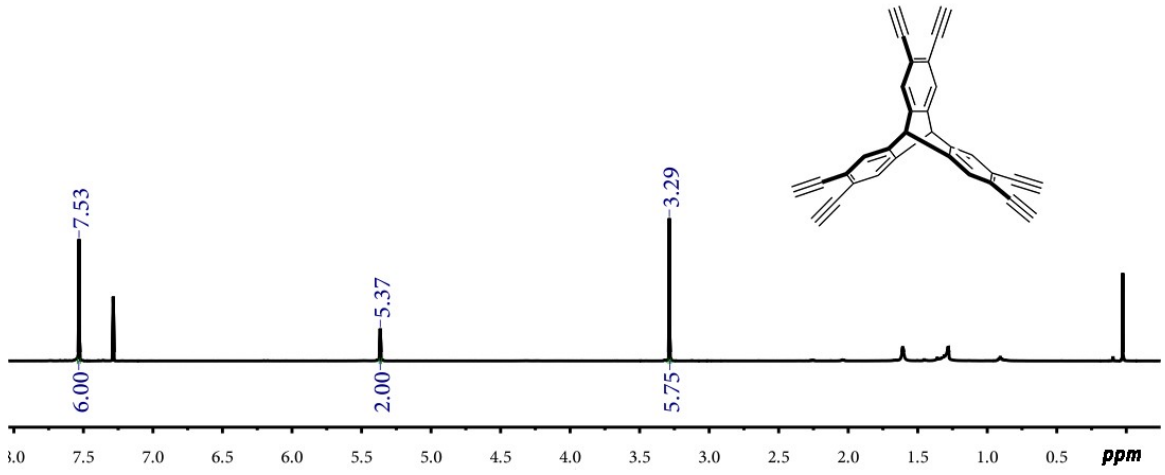

Fig. S3 ^{1}H NMR spectrum of 2,3,6,7,14,15- Hexaethynyltriptycene.

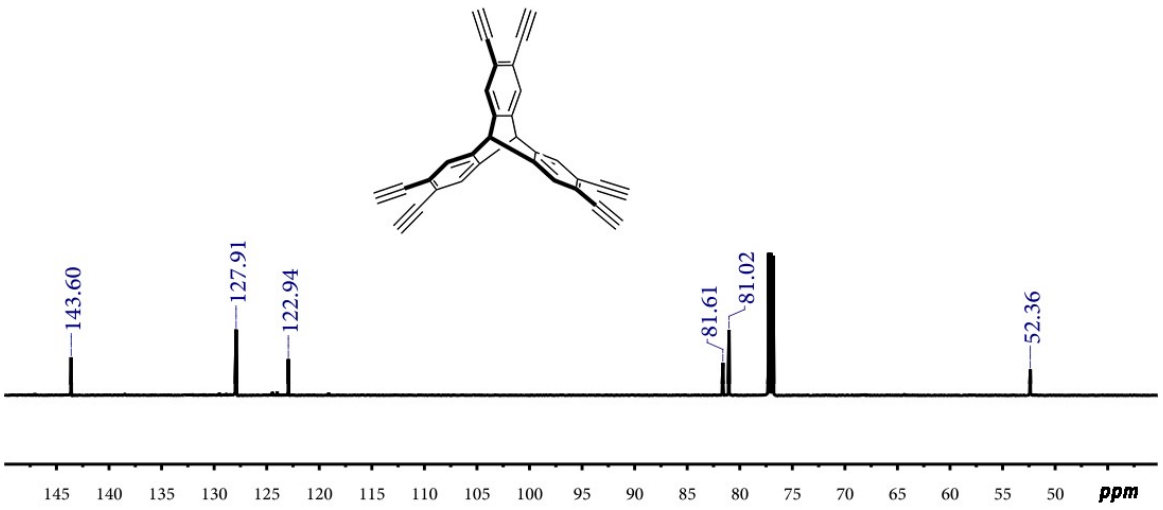

Fig. S4 ^{13}C NMR spectrum of 2,3,6,7,14,15- Hexaethynyltriptycene.

The characterization of G-PTN

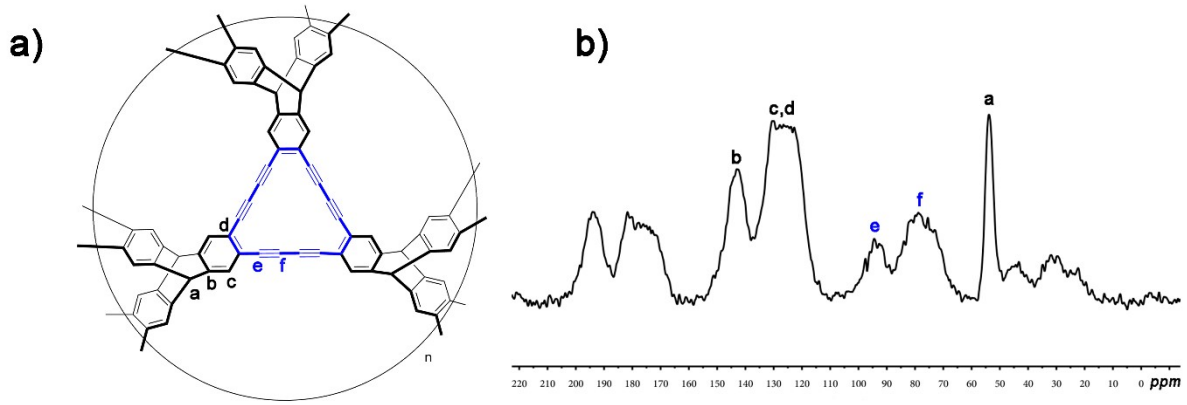

Fig. S5 Cross-polarization (CP) ^{13}C MAS NMR spectrum of G-PTN.

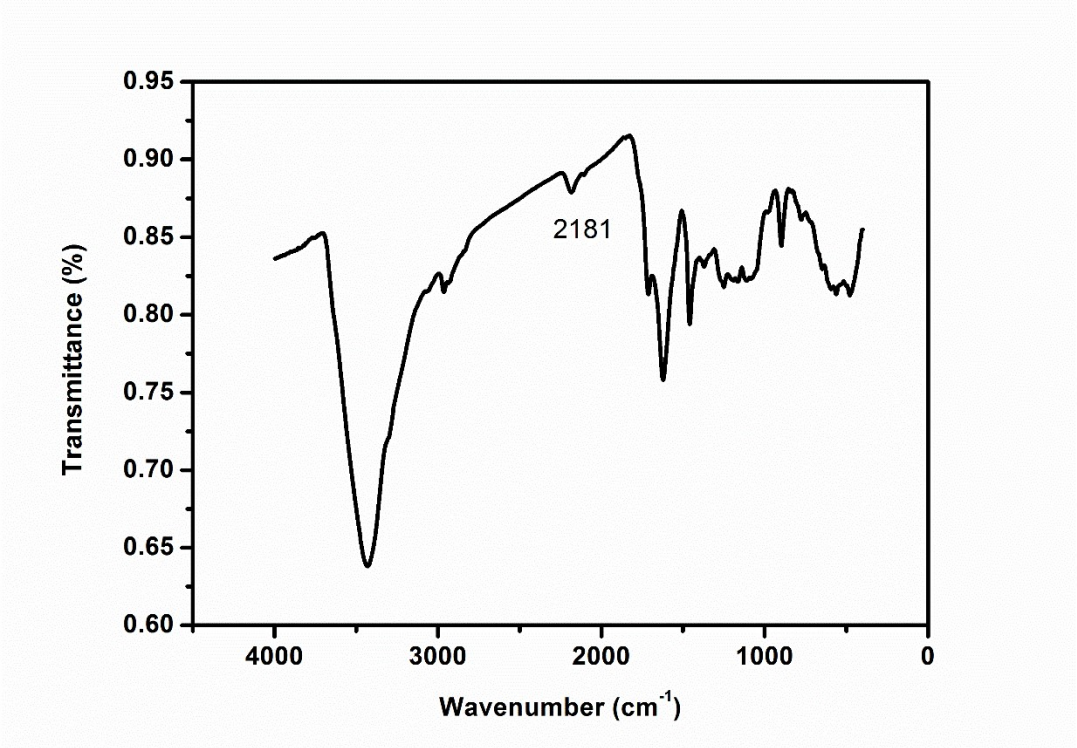

Fig. S6 FT-IR spectrum of G-PTN.

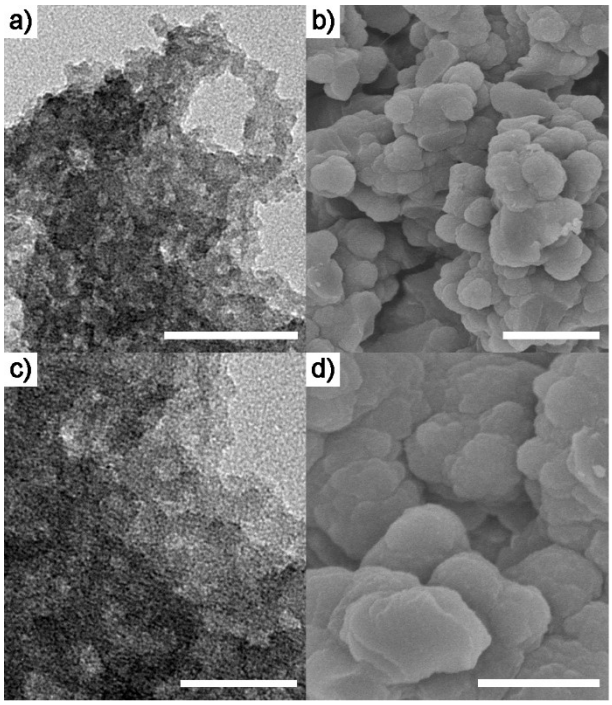

Fig. S7 Electron microscopy images of G-PTN. (a) and (c) Representative TEM images of G-PTN; (b) and (d) representative SEM images of G-PTN. Scale bar: 100 nm (a), 2 μm (b), 50 nm (c) and 1μm (d).

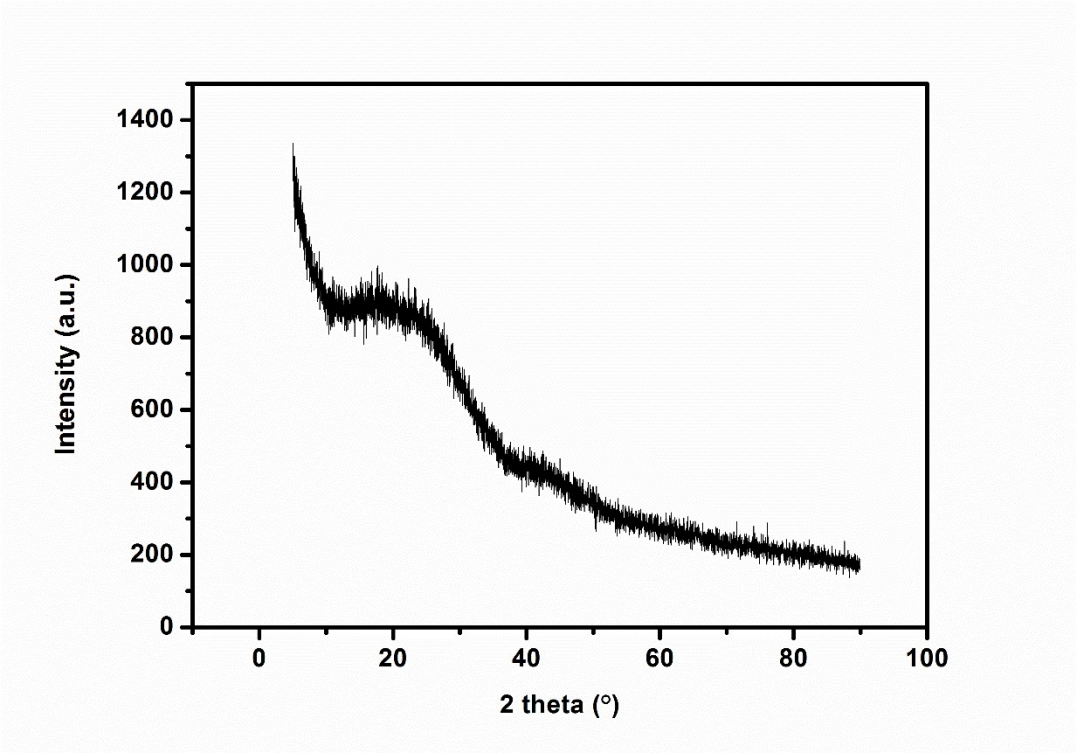

Fig. S8 Powder X-ray diffraction pattern of G-PTN.

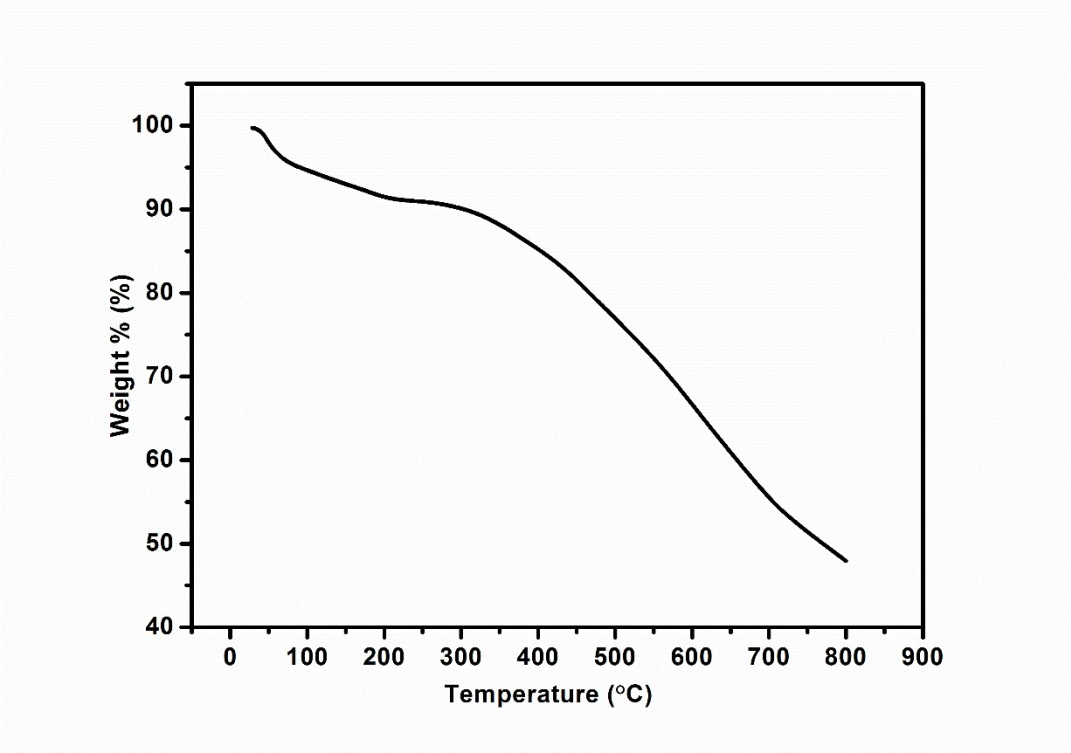

Fig. S9 TGA plot of G-PTN.

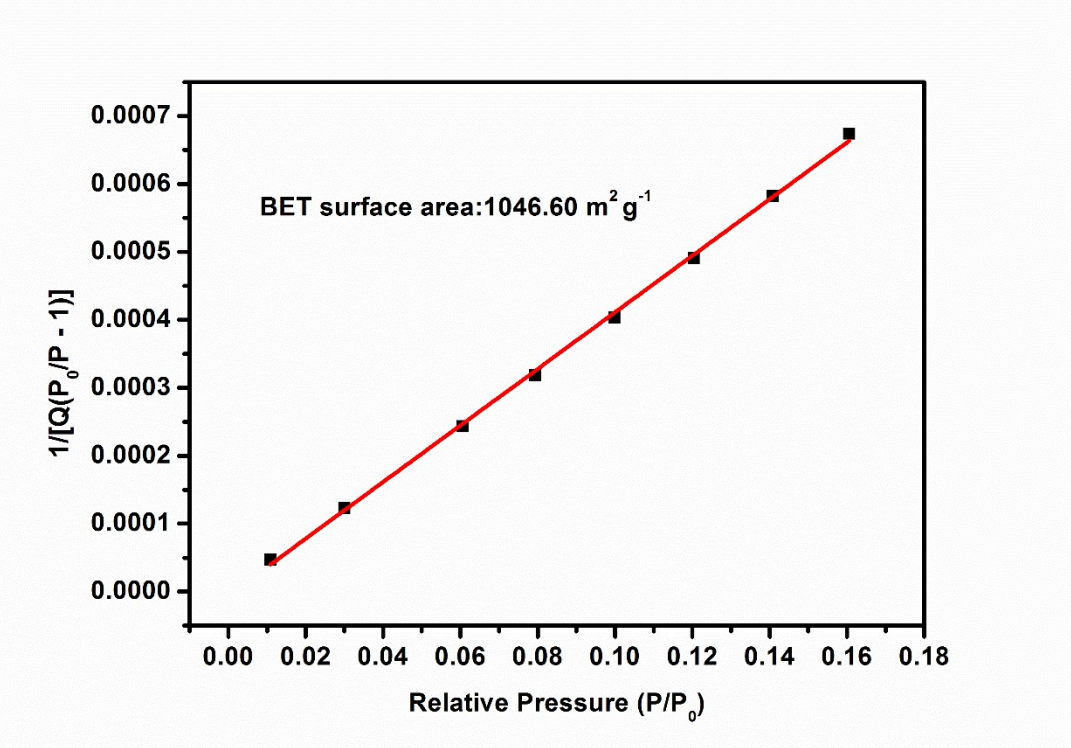

Fig. S10 BET surface area plot for G-PTN calculated from the nitrogen adsorption isotherm.

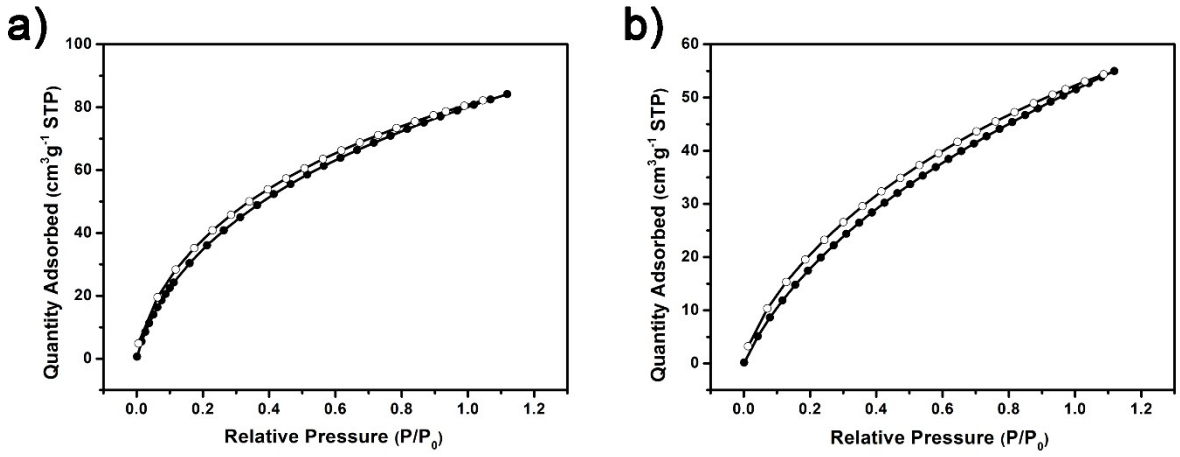

Fig. S11 CO_2 adsorption and desorption isotherms of G-PTN at (a) 273 K and (b) 298K. In (a) and (b), filled symbols denote gas adsorption and empty symbols denote desorption.

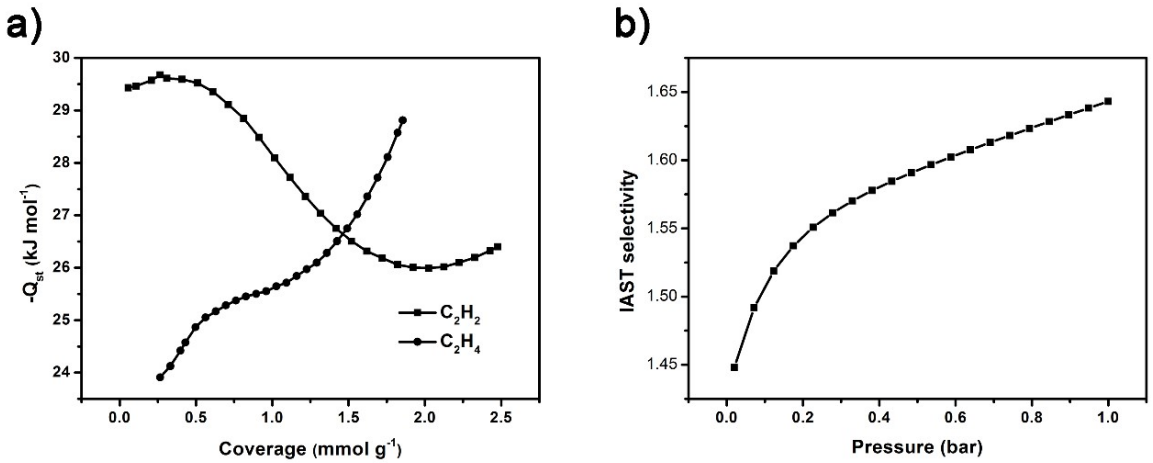

Fig. S12 (a) Isosteric heats of adsorption (Qst) for C_2H_2 and C_2H_4 in G-PTN; (b) predicted IAST selectivity values in gas mixture (1:99 v/v) of C_2H_2/C_2H_4 at 298 K.

The computation simulation based on model molecule M1

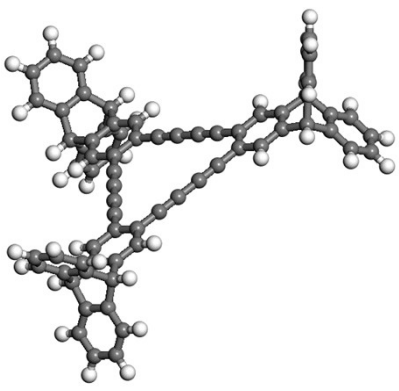

Fig. S13 The structure of the modle molecule M1.

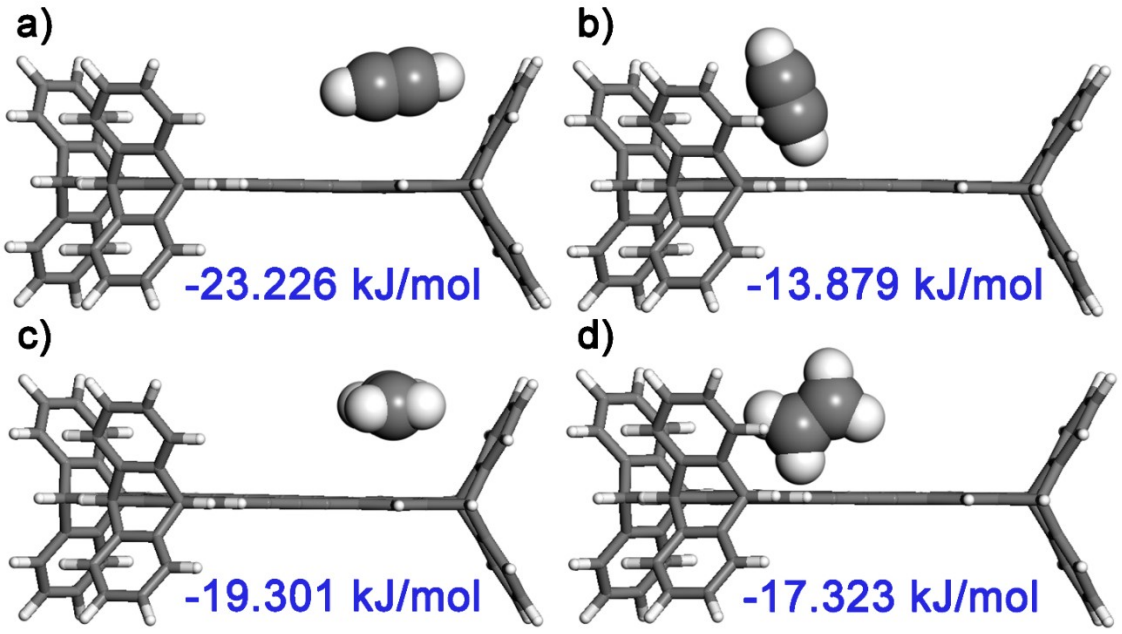

Fig. S14 The structures of binding configurations: (a) M1-$C_2H_2$1, (b) M1-$C_2H_2$2, (c) M1-$C_2H_4$1 and (d) M1-$C_2H_4$2. The binding energies calculated were also displayed in the figure.

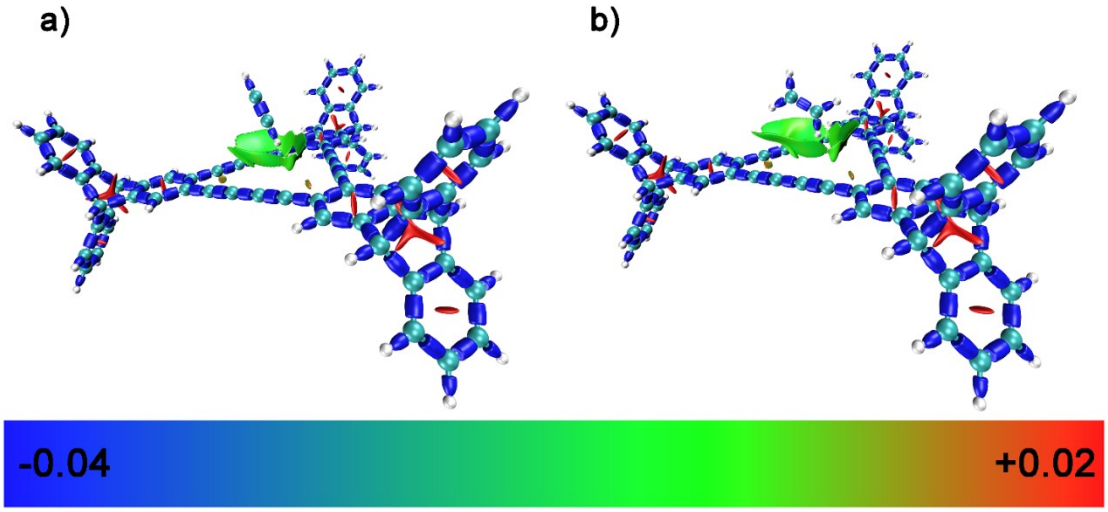

Fig. S15 Isosurface maps (IRI = 1.0) of configurations: (a) M1-$C_2H_2$2 and (b) M1-$C_2H_4$2. In (a) and (b), the isosurface was colored by the value of sign(λ2)ρ in BGR color model, where the blue regions represent notable attractions or chemical bonds, the green regions represent weak interactions like VDW interaction and the red regions represent notable repulsions like steric effect in ring.

The computation simulation based on triangular building units of graphdiyne

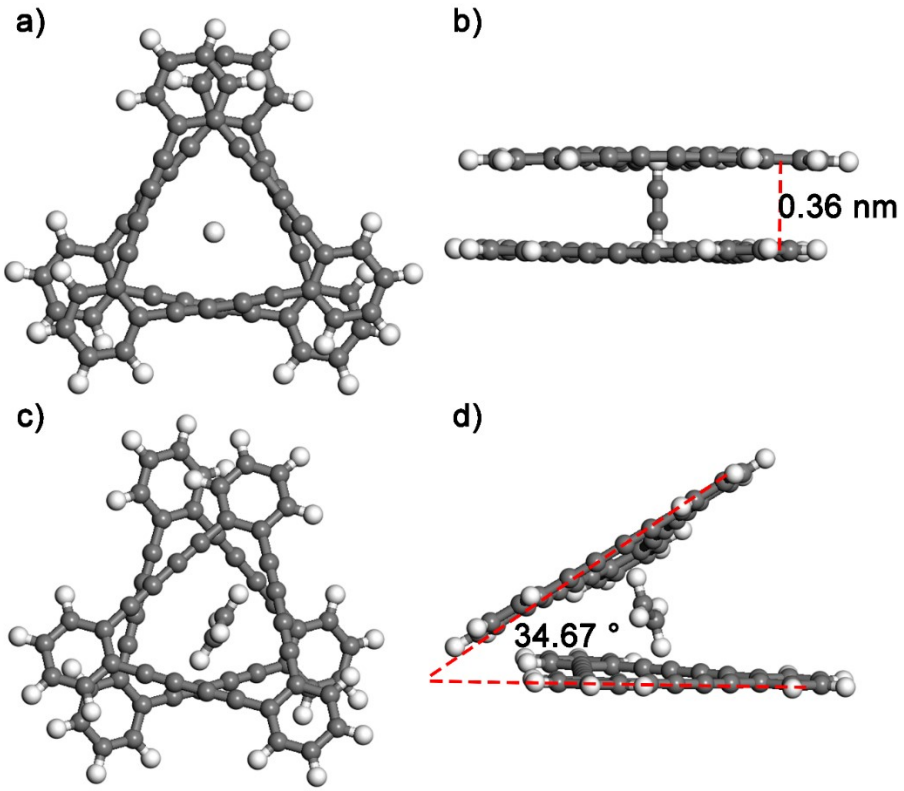

Fig. S16 The structures of binding configurations: (a) and (b) G2-$C_2H_2$1, (c) and (d) G2-$C_2H_4$1.

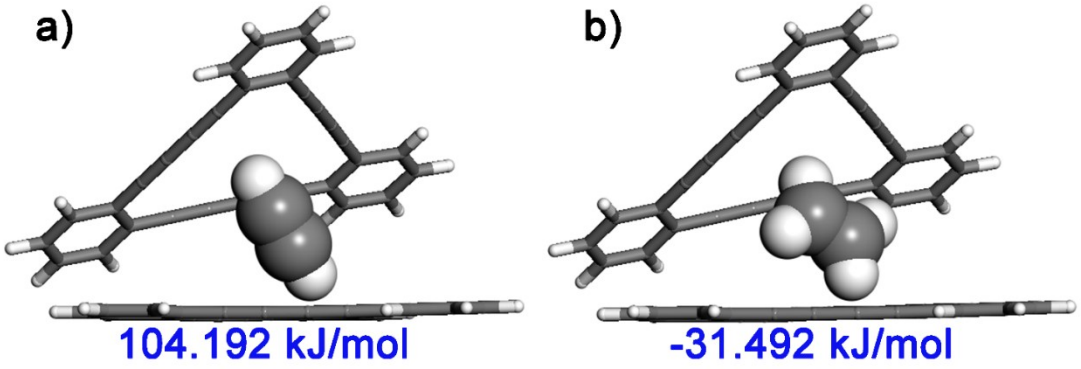

Fig. S17 The structures of binding configurations: (a) G2-$C_2H_2$2, (b) G2-$C_2H_4$1. The binding energies calculated were also displayed in the figure.

The computation simulation based on model molecule M2

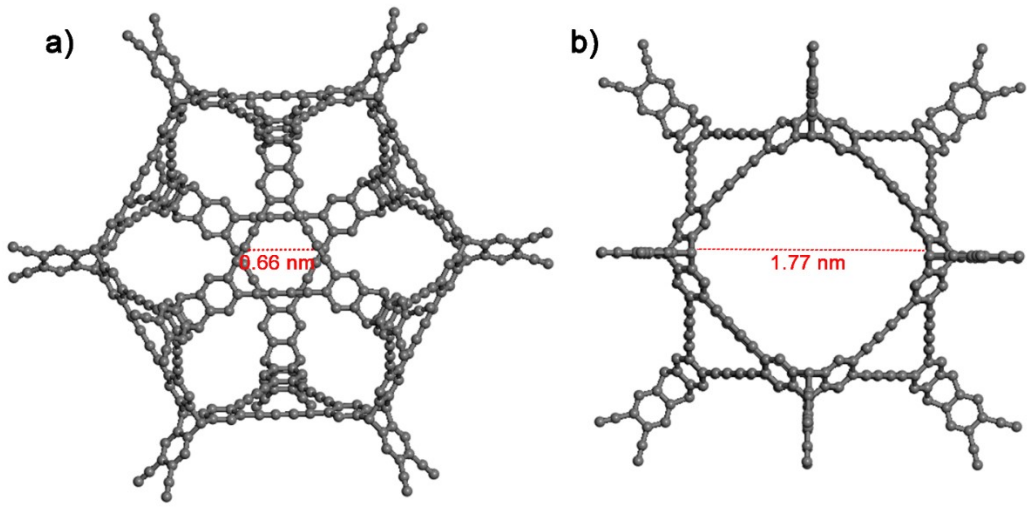

Fig. S18 The structure of M2. In (a) and (b), hydrogen atoms are omitted for clarity.

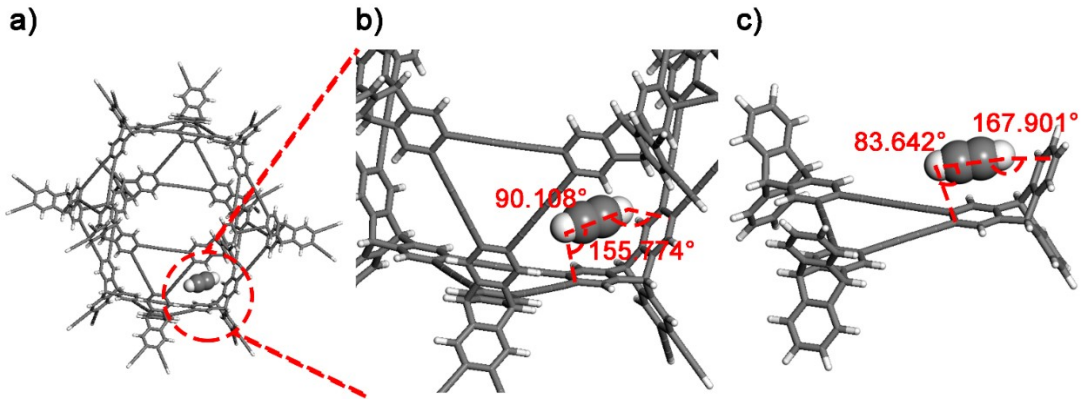

Fig. S19 The structure of configurations: (a), (b) M2-$C_2H_2$1 and (c) M1-C_2H_2com.